Particle acceleration by stimulated emission of radiation: Theory and experiment

Samer Banna,* Valery Berezovsky, and Levi Schächter
Department of Electrical Engineering, Technion, Israel Institute of Technology, Haifa 32000, Israel
(Received 28 June 2006; published 23 October 2006)

The interaction of electromagnetic radiation with free electrons in the presence of an active medium has some appealing outcomes. Among them is particle acceleration by stimulated emission of radiation (PASER). In its framework, energy stored in an active medium (microscopic cavities) is transferred directly to an *e*-beam passing through. We have developed a two-dimensional analytic model for the evaluation of the energy exchange occurring as a train of electron microbunches traverses a dilute resonant medium. Efficient interaction occurs at resonance—namely, when the frequency of the train matches the resonance frequency of the medium. It is shown that the energy exchange is γ independent for relativistic energies and it drops dramatically with an increase of the beam's radius. Based on this model, we have evaluated the relative change in the kinetic energy of a 0.1-nC 45-MeV macrobunch traversing an excited CO_2 gas mixture—the former being modulated at the CO_2 laser wavelength. Good agreement is found between the theoretical predictions and the results of the PASER experiment performed recently at Brookhaven National Laboratory.

DOI: 10.1103/PhysRevE.74.046501 PACS number(s): 29.17.+w, 41.75.-i, 41.60.Bq, 96.50.Pw

I. INTRODUCTION

It is well known that at the macroscopic level, an electron moving at a constant velocity in free space does not gain or lose energy. However, if the electromagnetic wake-field attached to this moving electron encounters a medium with characteristics different from the vacuum, the electron will experience a field scattered by the medium. As an example, let us briefly consider the interaction of a moving electron with three different media.

First, let us consider its motion along a vacuum channel embedded within a dielectric material. Provided that the electron's velocity exceeds the phase velocity of a plane wave in the medium, Čerenkov radiation is generated. What a remote observer measures as an electromagnetic energy comes at the expense of the electron's kinetic energy or, in other words, the electron is decelerated. Second, envision an electron moving in a vacuum channel within a lossy medium—a metallic structure characterized by a positive conductivity. In this case, the moving electron induces eddy currents in the metal. The heat generated by these currents comes at the expense of the electron's kinetic energy, and therefore, it is decelerated.

To have a better understanding of this deceleration force it is necessary to examine the electromagnetic wake-field distribution in the vicinity of the electron. Ignoring for a moment the presence of the *passive medium* (dielectric or metal), an electron generates in its rest frame of reference an electrostatic field, which transforms in the laboratory frame of reference into an infinite spectrum of evanescent waves—this field may be referred to as a *primary field*. As these waves hit the discontinuity between the vacuum channel and the medium, a so-called *secondary field* is generated. This field is actually the reaction of the medium to the presence of the electron. In both cases mentioned above, it is the action of this secondary field which decelerates the electron. Imagine now that we replace the passive medium by an *active medium* (negative conductivity)—this notion is conceived to represent a medium that amplifies radiation, contrary to a passive medium which causes radiation absorption. Subject to this substitution, the secondary field reverses its phase, leading to acceleration of the electron. In other words, energy stored in the medium may be transferred to the moving electron.

Motivated by the aforementioned third case, we now take a closer look at the interaction of charged particles with an active medium. For this purpose, let us consider an ensemble of atoms, each one being modeled by a two-level quantum system. As already indicated, the primary field consists of a broadband spectrum of evanescent waves—including the resonance frequency of this two-level system. These waves may be conceived as a spectrum of virtual photons continuously emitted and absorbed by the electron. When a virtual photon corresponding to the resonance frequency impinges upon an *excited* atom its effect is identical to that of a real photon. Therefore, it stimulates the atom, and as a result, two identical phase correlated photons are emitted. Being phase correlated, the stimulated photon can be absorbed by the moving electron, causing the latter's acceleration. The inverse process is also possible: if the virtual photon encounters an atom in the ground state and excites it, then the moving electron loses energy; i.e., the electron is decelerated. We may expect a nonzero net acceleration only if the number of atoms in the excited state is larger than that in the lower state; i.e., the population is inverted. From the description above, the acceleration force is a result of a stimulated radiation and accordingly the acronym PASER stands for particle acceleration by stimulated emission of radiation [1–7]. Obviously, efficient interaction occurs only in the close vicinity of the resonance. Therefore, from the perspective of a single

*Current address: Brookhaven National Laboratory, Upton, New York 11973, USA. Electronic address: sbanna@bnl.gov

 ©2006 The American Physical Society

moving electron, it is quite clear that since in the laboratory frame of reference its spectrum is broad, the effect of the medium on its energy is expected to be minuscule. In order to overcome this difficulty, it is suggested to inject a *train* of microbunches rather than a single macrobunch—its periodicity being identical to the resonance frequency of the medium. In this way, the projection of the train's spectrum on the resonance frequency of the medium becomes dominant.

It is instructive now to put this scheme in the correct perspective relative to the relevant acceleration concepts developed during the past two decades. These may be divided into several categories according to their driver. In the case of a laser wake-field acceleration (LWFA) [8–16] this is a short and intense laser pulse, for a plasma beat-wave accelerator (PBWA) [17] these are two long laser pulses oscillating at slightly different frequencies, and in the case of plasma wake-field acceleration (PWFA) [18–21] the driver is an intense electron pulse. Another acceleration scheme is the Čerenkov wake-field acceleration (CWFA) [22]. In this case, a driving bunch is injected into a vacuum tunnel of a dielectric loaded waveguide. The Čerenkov radiation generated by this bunch may be used to accelerate another bunch trailing behind. In all these acceleration schemes the primary energy is initially stored either in a laser pulse or in a driving bunch of electrons and it is eventually converted into an acceleration field.

In the framework of the PASER scheme, the primary energy is stored in an active medium and is transferred *directly* to the moving particles. In essence, this scheme may be conceived as the inverse of the Franck-Hertz effect. For the regime of the Franck-Hertz experiment [23]—namely, a *single* electron-atom collision (in average)—the phenomenon was demonstrated experimentally by Latyscheff and Leipunsky long ago (1930) [24]—this was the experimental evidence for collisions of the second kind. Yet the *accumulative* process has not been proven experimentally until recently [25].

Utilizing an active medium for particle acceleration suggests that this mechanism may be conceived as the *inverse laser* effect. In the past, a variety of mechanisms, which in natural conditions generate radiation, were considered for acceleration of particles. For example, in 1972 Palmer [26] suggested what is today well known as the inverse free-electron laser (I-FEL) [27,28]; Edighoffer *et al.* [29] suggested to use the inverse condition for Čerenkov radiation [30] to accelerate electrons, and Kroll conceived using the Smith-Purcell effect [31] for the same purpose [32].

Beyond the PASER basic concept [1], a series of novel phenomena associated with particle acceleration in an active medium were demonstrated theoretically [2,4–6]. It has been shown that the wake generated by a bunch of electrons may be amplified and the latter may be used subsequently to accelerate other electrons [2,6]. A unique instability has been demonstrated to occur when space-charge waves propagate in an active medium [5]. Furthermore, the equations of the interaction of an electromagnetic field with electrons in the presence of an active medium accounting for nonlinear effects have been developed and analyzed [4]. Our purpose in this study is to introduce a simple two-dimensional (2D) model for describing the interaction of a (finite-length) train of microbunches with an active medium.

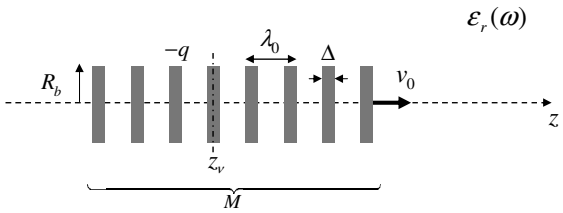

FIG. 1. A macrobunch consisting of a train of M microbunches traversing a medium characterized by its dielectric coefficient $\varepsilon_r(\omega)$. Each microbunch carries a charge $-q$.

The organization of the paper is as follows: the next section deals with the evaluation of the electromagnetic wake-field generated by a finite-length train of microbunches traversing a linear medium characterized by its scalar dielectric coefficient. In Sec. III the total energy emitted or absorbed by this train is calculated. We evaluate in Sec. IV the total energy absorbed by a train of microbunches as it traverses an active medium viewed as a two-level quantum system, accounting for the geometrical dimensions of the macrobunch. In Sec. V the potential energy exchange in a real system, considering the CO_2 gas mixture as an active medium, is determined and analyzed as practical estimates for the ongoing PASER experiment at the Brookhaven National Laboratory Accelerator Test Facility (BNL-ATF). A detailed description of the first experimental demonstration for the PASER scheme is presented in Sec. VI including a comparison of the experimental results with the theoretical predictions.

II. GENERAL FORMULATION OF THE WAKE-FIELD

In this section, we develop a general formulation of the wake-field generated by a train of electron microbunches traversing a dielectric medium characterized by a scalar dielectric coefficient $\varepsilon_r(\omega)$, which may be complex and frequency dependent.

Consider a macrobunch consisting of M microbunches, each one being azimuthally symmetric, having a radius R_b and a length Δ, carrying a charge $-q$ and moving at a constant velocity v_0, the distance between two adjacent microbunches being λ_0. We denote by z_ν the longitudinal coordinate of the center of the νth microbunch at $t=0$, as illustrated in Fig. 1. In the framework of this study, the medium is assumed to remain in the linear regime throughout the interaction region.

The moving train of microbunches generates a current density in the longitudinal direction (z axis) that is given in the time domain by

$$J_z(r,z;t) = -qv_0\sum_{\nu=1}^{M}\frac{1}{2\pi}\left[\frac{2}{R_b^2}h(R_b-r)\right] \times\left\{\frac{1}{\Delta}h\left[\frac{\Delta}{2}[z-(z_\nu+v_0t)]\right]\right\}, \tag{1}$$

where $h(\xi)$ is the Heaviside step function. In this expression it was tacitly assumed that each microbunch is uniformly distributed, and therefore, the transverse and longitudinal distributions are independent. Moreover, the particle's motion is confined to the z direction. The Fourier transform of this current density is

$$J_z(r,z;\omega) = -q\sum_{\nu=1}^{M}\frac{1}{(2\pi)^2}\left[\frac{2}{R_b^2}h(R_b-r)\right] \times\mathrm{sinc}\left(\frac{\omega\Delta}{2v_0}\right)\exp\left[-j\frac{\omega}{v_0}(z-z_\nu)\right], \tag{2}$$

wherein $\mathrm{sinc}(x)\equiv\sin(x)/x$.

This current density excites the z component of the magnetic vector potential which, in turn, satisfies the *inhomogeneous* wave equation. Hence, in the frequency domain, the magnetic vector potential is given by

$$A_z(r,z;\omega) = -\frac{\mu_0 q}{(2\pi)^2}\,\mathrm{sinc}\left(\frac{\omega\Delta}{2v_0}\right)\sum_{\nu=1}^{M}e^{-j(\omega/v_0)(z-z_\nu)}\times\begin{cases}\dfrac{2}{(\xi R_b)^2}[1-(\xi R_b)I_0(\xi r)K_1(\xi R_b)], & 0\le r\le R_b,\\ \dfrac{2}{\xi R_b}K_0(\xi r)I_1(\xi R_b), & R_b\le r<\infty,\end{cases} \tag{3}$$

with $\xi\equiv(\omega/\beta c)\sqrt{1-\beta^2\varepsilon_r(\omega)}$ and $\beta\equiv v_0/c$.

As we have determined the magnetic vector potential, the scalar electric potential may be calculated, resorting to Lorentz gauge and, accordingly, the longitudinal electric field in the frequency domain is given by

$$E_z(r,z;\omega) = -j\omega\left[1-\frac{1}{\beta^2\varepsilon_r(\omega)}\right]A_z(r,z;\omega) \tag{4}$$

or, in the time domain,

$$E_z(r,z;t) = \frac{\mu_0 q}{(2\pi)^2}\sum_{\nu=1}^{M}\int_{-\infty}^{\infty}d\omega(j\omega)\left[1-\frac{1}{\beta^2\varepsilon_r(\omega)}\right]\times\exp\left\{j\omega\left[t-\frac{(z-z_\nu)}{v_0}\right]\right\}\mathrm{sinc}\left(\frac{\omega\Delta}{2v_0}\right) \times\begin{cases}\dfrac{2}{(\xi R_b)^2}[1-(\xi R_b)I_0(\xi r)K_1(\xi R_b)], & 0\le r\le R_b,\\ \dfrac{2}{(\xi R_b)}K_0(\xi r)I_1(\xi R_b), & R_b\le r<\infty.\end{cases} \tag{5}$$

Since the only component of the current density is in the z direction, it is sufficient to evaluate the longitudinal component of the electric field in order to establish the energy exchange in the system. The latter is determined by the product $\vec{J}\cdot\vec{E}$, as dictated by Poynting's theorem.

III. ENERGY EXCHANGE OF A TRAIN IN A MEDIUM

Utilizing the term for the longitudinal electric field as determined in Eq. (5), the expression for the current density [Eq. (1)], and integrating the power density over the beam's volume,

$$P(t) = -2\pi\int_0^{\infty}drr\int_{-\infty}^{\infty}dz\,J_z(r,z;t)E_z(r,z;t), \tag{6}$$

we obtain the total power exchanged in the interaction process. This quantity is negative if an electromagnetic power is absorbed by the train and is positive if an electromagnetic power is generated at the expense of the train's kinetic energy. Explicitly, the power exchange reads

$$P = \frac{\eta_0\beta q^2}{(2\pi)^2}\int_{-\infty}^{\infty}d\omega j\omega\left[1-\frac{1}{\beta^2\varepsilon_r(\omega)}\right]\frac{2}{u^2}[1-2I_1(u)K_1(u)] \times\mathrm{sinc}^2\left(\frac{\omega\Delta}{2v_0}\right)\sum_{\nu'=1}^{M}\sum_{\nu=1}^{M}e^{-j(\omega/v_0)(z_{\nu'}-z_\nu)}, \tag{7}$$

where $z_\nu=z_1+(\nu-1)\lambda_0$, $\nu=1,2,\ldots,M$, $u\equiv\xi R_b$, and η_0 is the free-space wave impedance. The double averaging over the longitudinal initial location of the microbunches may be simplified to read

$$\sum_{\nu'=1}^{M}\sum_{\nu=1}^{M} e^{-j(\omega/v_0)(z_{\nu'}-z_\nu)} = M^2 \frac{\mathrm{sinc}^2\left(\frac{\omega}{2v_0}\lambda_0 M\right)}{\mathrm{sinc}^2\left(\frac{\omega}{2v_0}\lambda_0\right)}, \tag{8}$$

and accordingly, the total power exchange is given by

$$P = \frac{\eta_0 \beta Q^2}{(2\pi)^2}\int_{-\infty}^{\infty} d\omega j\omega\left[1-\frac{1}{\beta^2\varepsilon_r(\omega)}\right]\times\frac{2}{u^2}[1-2I_1(u)K_1(u)]$$

$$\times \mathrm{sinc}^2\left(\frac{\omega\Delta}{2v_0}\right)\frac{\mathrm{sinc}^2\left(\frac{\omega}{2v_0}\lambda_0 M\right)}{\mathrm{sinc}^2\left(\frac{\omega}{2v_0}\lambda_0\right)}, \tag{9}$$

Q ($\equiv Mq$) being the total charge in the macrobunch.

It is convenient to introduce a set of normalized quantities as follows:

$$\bar{\Delta} \equiv \frac{\Delta}{\lambda_0}, \quad \bar{R}_b \equiv \frac{R_b}{\lambda_0}, \quad \Omega \equiv \omega\frac{\lambda_0}{c},$$

$$\psi \equiv \frac{\Omega}{2\beta}, \quad u \equiv \frac{\Omega\bar{R}_b}{\beta}\sqrt{1-\beta^2\varepsilon_r(\Omega)}, \tag{10}$$

and define the longitudinal and transverse form factors of the beam as

$$F_\parallel(\psi,\bar{\Delta},M) \equiv \mathrm{sinc}^2(\psi\bar{\Delta})\frac{\mathrm{sinc}^2(\psi M)}{\mathrm{sinc}^2(\psi)},$$

$$F_\perp(u) \equiv \frac{2}{u^2}[1-2I_1(u)K_1(u)]. \tag{11}$$

Based upon these definitions, the total power exchange is given by

$$P = \frac{Q^2 v_0}{4\pi\varepsilon_0\lambda_0^2}\frac{2}{\pi}\int_0^\infty d\Omega\, F_\parallel(\psi,\bar{\Delta},M)$$

$$\times \mathrm{Re}\left\{j\Omega\left[1-\frac{1}{\beta^2\varepsilon_r(\Omega)}\right]F_\perp(u)\right\}. \tag{12}$$

Note that the argument u may be real, pure imaginary, or complex according to the frequency dependence of $\varepsilon_r(\Omega)$, as well as to the value of β.

Assuming that the length of the macrobunch is shorter than the interaction length ($d \gg M\lambda_0$) and ignoring edge effects, the energy exchange during the passage ($T=d/v_0$) is given by

$$W = \frac{Q^2 d}{4\pi\varepsilon_0\lambda_0^2}\frac{2}{\pi}\int_0^\infty d\Omega\, F_\parallel(\psi,\bar{\Delta},M)$$

$$\times \mathrm{Re}\left\{j\Omega\left[1-\frac{1}{\beta^2\varepsilon_r(\Omega)}\right]F_\perp(u)\right\}. \tag{13}$$

In the next section we use this result in order to evaluate the energy exchange when the train of bunches moves in an active medium. However, before doing so it is instructive to examine a more familiar case: namely, a plain dielectric medium. If the macrobunch is moving with a speed below the Čerenkov velocity—i.e., $\beta<\beta_{\mathrm{Ce}}\equiv 1/\sqrt{\varepsilon_r}$, where ε_r is real and frequency independent—it is obvious that in such a case u is real and so is $F_\perp$, implying that $\mathrm{Re}\{(j\Omega)\ldots\}=0$ and, as expected, no radiation is generated or absorbed ($W=0$).

If v_0 exceeds the Čerenkov velocity—i.e., $\beta>\beta_{\mathrm{Ce}}$—then u is pure imaginary, entailing [33] $I_1(ju)=jJ_1(u)$ and $K_1(ju)=-(\pi/2)H_1^{(2)}(u)$ with $u\equiv\Omega\bar{R}_b/\beta\sqrt{\beta^2\varepsilon_r-1}$. Consequently, $\mathrm{Re}[jF_\perp(u)]=(\pi/2)J_c^2(u)$ wherein $J_c(u)\equiv 2J_1(u)/u$ and

$$W^{(\mathrm{Ce})} = \frac{Q^2 d(\beta^2\varepsilon_r-1)}{4\pi\varepsilon_0\varepsilon_r\lambda_0^2\beta^2}\int_0^\infty d\Omega\,\Omega F_\parallel(\psi,\bar{\Delta},M)$$

$$\times J_c^2\left(\frac{\Omega\bar{R}_b}{\beta}\sqrt{\beta^2\varepsilon_r-1}\right). \tag{14}$$

It is worth indicating that the longitudinal form factor ($F_\parallel$) and $J_c^2(x)$ are positive terms. Hence, the total energy exchange is positive, indicating that energy is emitted at the expense of the kinetic energy of the bunch.

Moreover, assuming a real frequency dependent dielectric coefficient, the total energy exchange, as given in Eq. (13), for a point charge (i.e., a single electron) as it traverses the dielectric medium reads

$$W = \frac{e^2 d}{4\pi\varepsilon_0\lambda_0^2}\int_{\beta\sqrt{\varepsilon_r(\Omega)}>1} d\Omega\,\Omega\left[1-\frac{1}{\beta^2\varepsilon_r(\Omega)}\right], \tag{15}$$

where it was assumed that $\bar{R}_b\to 0$, $\bar{\Delta}\to 0$, and $M=1$. The last integral coincides with the typical expression for the total energy radiated by an electron as a function of the path d, as first calculated by Frank and Tamm [34].

IV. ENERGY EXCHANGE IN AN ACTIVE MEDIUM

Based on the expressions for the energy exchange taking place in a linear dielectric medium, as established in the preceding section, we evaluate in this section the energy exchange in an active medium, the latter being represented by a scalar dielectric function

$$\varepsilon_r(\omega>0) \equiv 1+\frac{\omega_p^2}{\omega_0^2-\omega^2+2j\omega/T_2} \tag{16}$$

and subject to the condition $\varepsilon_r(\omega<0)=\varepsilon_r^*(\omega>0)$. It is tacitly assumed that the medium has a single resonance frequency ω_0 chosen to correspond to the macrobunch modulation—i.e., $\omega_0=2\pi c/\lambda_0$; $\omega_p^2\equiv e^2 n/m\varepsilon_0$ is the "plasma" frequency, with m being the rest mass of the electron and n representing the population density of the resonant atoms (or molecules). For an excited medium, when the relevant population density is inverted, the plasma frequency is negative ($\omega_p^2<0$), T_2 being the relaxation time.

The density of the energy stored in the medium at the resonance frequency, assuming its population is inverted (n is negative), is given by

$$w_{\mathrm{act}} = -n\hbar\omega_0, \tag{17}$$

where $\hbar = 1.05457 \times 10^{-34}$ [J sec] is the Plank constant; using the preceding definitions,

$$\varepsilon_r(\Omega > 0) \equiv 1 + \frac{\Omega_p^2}{(2\pi)^2 - \Omega^2 + 2j\alpha\Omega}, \tag{18}$$

wherein $\alpha \equiv \lambda_0 / cT_2$ and $\Omega_p^2 \equiv \omega_p^2 \lambda_0^2 / c^2$.

With the description of the medium accomplished, it is possible to evaluate analytically the integral in Eq. (13) subject to two assumptions: (i) the bandwidth associated with the frequency response of the medium is much narrower than the spectrum associated with the finite-length of the macrobunch ($M\alpha \ll 1$). In other words, the frequency response of the medium is sharper than the longitudinal form factor. (ii) The bandwidth of the resonance is very narrow compared to the resonance itself—i.e., $\alpha \ll \Omega_0$ $(=2\pi)$. Based on these assumptions, we can take the longitudinal form factor out of the integral [Eq. (13)] and evaluate the latter only at the poles of the dielectric function

$$\varepsilon_r(\Omega) = 0, \tag{19}$$

namely, $\Omega = \Omega_\pm \equiv j\alpha \pm \sqrt{(2\pi)^2 + \Omega_p^2 - \alpha^2} \equiv j\alpha \pm \Omega_R$, by using the Cauchy residue theorem; the result reads

$$W \simeq \frac{Q^2 d}{4\pi\varepsilon_0 \lambda_0^2 \beta^2} \frac{\Omega_p^2}{\Omega_R} F_\parallel\left(\frac{\Omega_R}{2\beta}, \bar{\Delta}, M\right) \mathrm{Re}\left[\Omega_+ F_\perp\left(\frac{\Omega_+ \bar{R}_b}{\beta}\right)\right]. \tag{20}$$

In order to gain some insight regarding the impact of the various parameters on the energy exchange, we consider a realistic regime and assume $\gamma \gg 1$ $\left(\gamma \equiv \frac{1}{\sqrt{1-\beta^2}}\right)$, $|\Omega_p^2| \ll (2\pi)^2$, and $\alpha^2 \ll (2\pi)^2$. Accordingly, the last expression may be approximated to read

$$W \simeq \frac{Q^2 d}{4\pi\varepsilon_0 \lambda_0^2} \Omega_p^2 \,\mathrm{sinc}^2(\pi\bar{\Delta}) \mathrm{sinc}^2\left(\frac{\pi M}{2\gamma^2}\right) F_\perp(2\pi\bar{R}_b). \tag{21}$$

Evidently, the total energy exchange is proportional to Ω_p^2. Consequently, as the population in the medium is inverted, Ω_p^2 is negative and so is the term for W, indicating that energy is transferred from the active medium to the macrobunch, and accordingly, electrons are accelerated. Therefore, the total gain in the kinetic energy of the macrobunch ($\Delta E_k \equiv -W$) is positive. Moreover, we observe that the energy exchange vanishes if the macrobunch is not modulated ($\bar{\Delta} = 1$), and if $\gamma^2 \gg M$, the energy exchange is M independent, implying that each microbunch may interact independently with the medium.

Now, let us determine the relative change in the kinetic energy of the macrobunch. Denoting by N_{el} the total number of electrons in the macrobunch (i.e., $Q = N_{\mathrm{el}} e$), the relative change in the kinetic energy ($\overline{\Delta E_k}$) reads

$$\overline{\Delta E_k} \equiv \frac{\Delta E_k}{N_{\mathrm{el}} mc^2(\gamma - 1)} = \frac{4N_{\mathrm{el}} d(\pi r_e^2)}{\beta^2(\gamma - 1)} \frac{1}{\Omega_R} \frac{w_{\mathrm{act}}}{\hbar\omega_0} \times F_\parallel\left(\frac{\Omega_R}{2\beta}, \bar{\Delta}, M\right) \mathrm{Re}\left[\Omega_+ F_\perp\left(\frac{\Omega_+ \bar{R}_b}{\beta}\right)\right], \tag{22}$$

wherein we have used the definition in Eq. (17) and $r_e \equiv e^2 / 4\pi\varepsilon_0 mc^2$ is the classical radius of the electron. In a similar manner, the relative change in the kinetic energy, subject to the assumptions of Eq. (21), reads

$$\overline{\Delta E_k} = \frac{4N_{\mathrm{el}} d(\pi r_e^2)}{(\gamma - 1)} \frac{w_{\mathrm{act}}}{\hbar\omega_0} \mathrm{sinc}^2(\pi\bar{\Delta}) \mathrm{sinc}^2\left(\frac{\pi M}{2\gamma^2}\right) F_\perp(2\pi\bar{R}_b). \tag{23}$$

Note that the last quantity is positive when the population is inverted ($w_{\mathrm{act}} > 0$).

Equations (22) and (20) together are the essence of the theoretical part of this study, as they determine the energy exchange occurring as a finite-length train of microbunches traversing an active medium, accounting for the geometry of the microbunches.

V. TRAIN IN AN ACTIVE CO_2 GAS MIXTURE

The analysis presented above was the basis for the design of the proof-of-principle PASER experiment. In this section, we present the main considerations in the design process with special emphasis on the optimization of the energy exchange.

A. Mixture pressure

The availability of the high-power CO_2 laser in conjunction with the 70-MeV linac at the BNL-ATF dictates to a large extent the choice of the wavelength ($\lambda_0 = 10.2$ μm). Obviously, this determines the gas mixture to be used, and the next step would be to determine its pressure. The latter is a compromise between two constraints: high pressure (10–30 atm) may pose a significant difficulty since a thick window would be necessary to sustain the pressure gradient between the gas cell and the accelerator beam pipe. Such a window may affect dramatically the emittance of the e-beam. Furthermore, utilizing the small-angle approximation to multiple Coulomb scattering [39] it is evident that the scattering angle of the e-beam increases as the gas pressure increases and it is inversely proportional to the electron momentum. Hence, for higher pressures thicker windows are needed, and therefore, scattering from the windows, as well as from the gas, starts to play a more significant role. Moreover, as the refractive index of the gas increases, so does the emission of the Čerenkov radiation which, in turn, may lead to a reduction of the PASER mechanism. On the other hand, a choice of a very low pressure entails minuscule energy stored in the medium and thus a negligible interaction.

As a trade-off between these conflicting trends we have found that a fraction of atmosphere (0.25 atm) is a reasonable compromise, enabling to store up to 200 mJ/cm^3 in the medium. In addition to the amount of stored energy, by

choosing the pressure we also determine to a large extent the bandwidth of the resonance. A typical value for the transverse relaxation time at such a pressure is $T_2=2$ nsec [35], and hence, the assumption $M\alpha \ll 1$ is valid for macrobunches consisting of 1000 microbunches at the most (i.e., $M<1000$). It is noteworthy that for such a pressure and for 45-MeV e-beam the scattering angle from the PASER cell (windows and gas mixture) as given by the Lynch-Dahl approximation [39] is less than 3 mrad.

B. Resonance selection

While the choice of wavelength was set by the availability of instrumentations, the selection of the resonances in the excited medium is controlled by the medium bandwidth and the train's pulse duration. Thus far, a single resonance was considered. However, one should bear in mind that, in practice, any medium has multiple resonances. As already indicated, the bandwidth of the medium is determined by the pressure, so we do not have this degree of freedom, but we may affect the spectrum of the train by varying the number of microbunches (M). Denoting by $\Delta\Omega$ the normalized frequency difference between the operating resonance frequency (Ω_0) and the nearest adjacent resonant frequency of the medium, it is obvious that for a proper frequency selection, the number of microbunches ought to be large—i.e., $M \gg 1/\Delta\Omega$ [see Eq. (8)]. Combining the last condition with the assumption that $M\alpha \ll 1$ entails the following condition:

$$\alpha \ll \frac{1}{M} \ll \Delta\Omega. \tag{24}$$

In a realistic CO_2 gas mixture the nearest adjacent resonance frequency corresponds to 9.2 μm, and therefore, the normalized frequency difference is $\Delta\Omega/2\pi=0.1$. Accordingly, for any practical purposes, the single-resonance approximation is valid for macrobunches consisting of more than 50 microbunches—corresponding to a pulse duration of 1.6 [psec]. In principle, the pulse duration could be varied from 1 to 5 psec.

The impact of the pulse duration on the frequency selection is illustrated in Fig. 2 where we plot the longitudinal form factor [Eq. (11)] as a function of the normalized frequency Ω/Ω_0, assuming $\Delta=0.1\lambda_0$, while M is a parameter ($M=5,10,30,80$), and $\Omega=1.1\Omega_0$ corresponds to the nearest adjacent resonance frequency. Evidently, for $M>30$ the single-resonance-frequency approximation is fully justified.

C. Energy density stored in the medium

In the case of collective effects [3], it is well known that not only the amplitude of the electromagnetic field is affected by the interaction but also its phase. As a result, the effective phase of the wake-field relative to the microbunch may change, and therefore, the interaction may diminish. In other words, we may expect the energy exchange to be zero for low energy stored in the medium and to diminish again for relatively high values of the energy density. In between, the energy exchange is expected to reach a peak value. Since the energy exchange is linearly

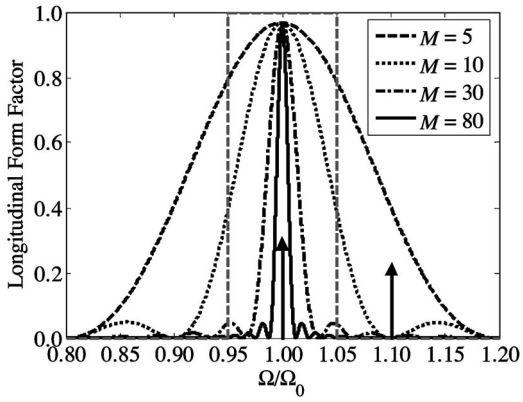

FIG. 2. The longitudinal form factor versus the normalized frequency with M as a parameter ($\Delta=0.1\lambda_0$). $\Omega=\Omega_0$ corresponds to the main resonance frequency, while $\Omega=1.1\Omega_0$ corresponds to the nearest adjacent resonance frequency in a CO_2 gas mixture. The microbunch length ($\Delta=0.1\lambda_0$) determines the maximum value of the longitudinal form factor.

proportional to the interaction length (d), in the following examples, an interaction length of 0.5 m is assumed.

Figure 3 illustrates the relative change in the kinetic energy of the macrobunch versus the energy density stored in the excited CO_2 gas mixture at the resonance frequency. In frame (a) this quantity is presented for different e-beam radii and $M=90$, while in frame (b) the relative change is presented for different values of M and $R_b=10\lambda_0$. In both cases, the average kinetic energy of the electrons $[E_k=mc^2(\gamma-1)]$ was taken to be 45 MeV and each microbunch is of $0.1\lambda_0$ length; the macrobunch consists of $N_{el}=10^{10}$ electrons. Both frames show that $\overline{\Delta E_k}$ oscillates as a function of w_{act}. These oscillations are a by-product of the functional behavior of the longitudinal form factor of the macrobunch [Eq. (11)]. Specifically, the energy densities for which the relative change vanishes correspond to the zero points of the longitudinal form factor—i.e., $w_{act}: \psi_R=\nu\pi$, where ν is an integer.

Denoting by $w_{act}^{(opt)}$ the energy density that maximizes the relative change in the kinetic energy of the macrobunch, we observe that this quantity is R_b independent and it increases with a decrease of M. As one may expect, keeping the amount of charge in the macrobunch constant along with increasing the e-beam radius, the charge density in the macrobunch decreases, and therefore, the optimal relative change in the kinetic energy drops—see Fig. 3(a). In a similar way, increasing the number of microbunches while keeping the total charge in the macrobunch unchanged, the total amount of charge in each single microbunch decreases, and as a result, the peak of the relative change in the kinetic energy decreases—as revealed in Fig. 3(b).

D. Initial kinetic energy dependence

Any viable acceleration scheme must exhibit that its energy gain is independent of the initial kinetic energy—in the relativistic regime. Frame (a) of Fig. 4 presents this gain for different macrobunch pulse durations corresponding to $M=60,90,120,150$; the energy density stored in the medium

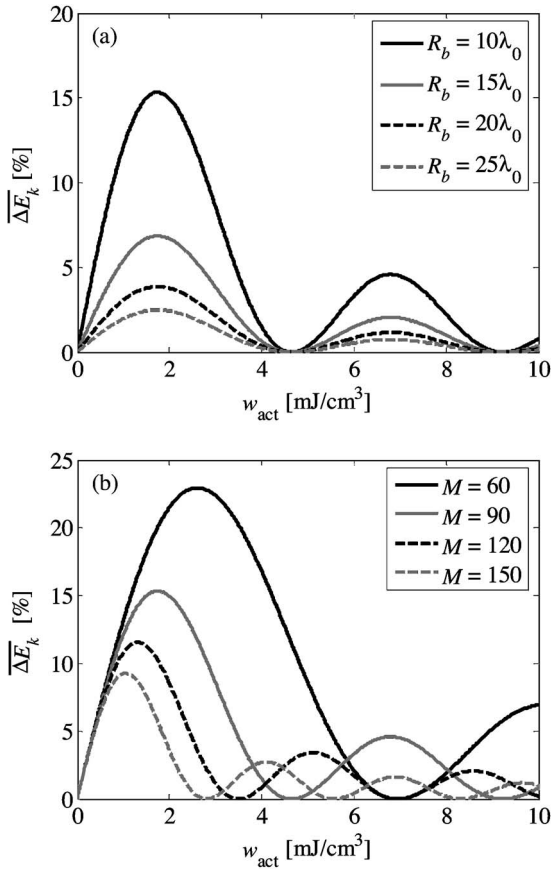

FIG. 3. The relative change in the kinetic energy of the macrobunch versus the energy density stored in the medium at the resonance frequency. Each single electron has a kinetic energy of 45 MeV, the microbunch length is set to be $\Delta=0.1\lambda_0$, and $N_{el}=10^{10}$. (a) The e-beam's radius is a parameter, while $M=90$. (b) The number of microbunches is a parameter, while $R_b=10\lambda_0$.

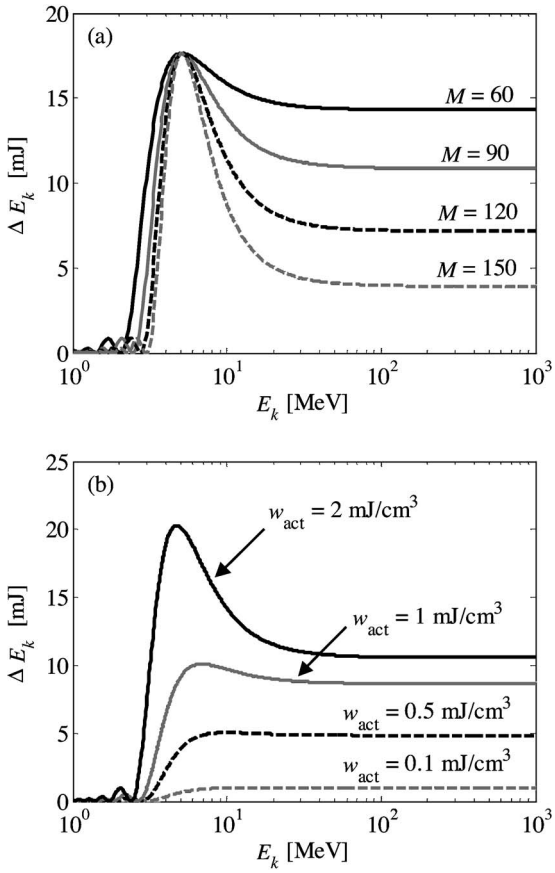

FIG. 4. The macrobunch kinetic energy increase versus the average kinetic energy of the electrons. The macrobunch radius is $10\lambda_0$, and the microbunch length is $0.1\lambda_0$, and $N_{el}=10^{10}$. (a) The number of microbunches is a parameter, and $w_{act}=1.7$ mJ/cm^3. (b) The energy density stored in the medium at the resonance is a parameter with $M=90$.

was chosen to correspond to the optimal relative change (at $M=90$) as revealed in Fig. 3(a)—i.e., $w_{act}=1.7$ mJ/cm^3. The dependence on the latter quantity is introduced in frame (b) where w_{act} is a parameter and $M=90$. In both cases, $R_b=10\lambda_0$ and $\Delta=0.1\lambda_0$. As a reference value, the total kinetic energy of a 45-MeV macrobunch consisting of 10^{10} electrons is 72 mJ.

Three facts are evident from Fig. 4. First, as expected of any acceleration scheme, the increase in the kinetic energy of the e-beam is γ independent for relativistic electrons. In the experiment, the electrons' energy (45 MeV) was dictated by the availability of the wiggler which modulates the electrons—therefore, we operated in the regime where the energy exchange was γ independent. Second, the kinetic energy gain peaks as a function of γ. The optimal kinetic energy where the energy gain peaks, denoted by $E_k^{(opt)}$, is M independent and approaches lower values as the energy density stored in the medium increases towards $w_{act}^{(opt)}$. Third, as revealed in frame (a), the peak of the kinetic energy gain (at low energies) is not affected by the amount of charge in the microbunch but rather by the geometry of the latter (R_b and Δ). Moreover, this optimal gain is strongly controlled by the energy density stored in the medium at the resonance frequency.

E. Bunch configuration

Let us now examine the impact of the bunch's parameters: the length of each single microbunch (Δ) and their number (M), keeping the charge in the macrobunch constant ($N_{el}=10^{10}$); the effect of the radius has been examined in the context of Fig. 3(a).

In Fig. 5(a) we show the kinetic energy gain versus the length of a single microbunch, while the beam radius (R_b) is a parameter. The other parameters are $M=90$, $E_k=45$ MeV, and $w_{act}=1.7$ mJ/cm^3. Obviously, the energy gain vanishes as the length of the microbunch approaches the modulation wavelength and it reaches a maximum for the shortest bunch. In practice, the length of the microbunch is limited primarily by the modulation process and by the space-charge effects within the microbunch. As will be discussed in the next section, the drift region between the wiggler, where the e-beam velocity is modulated, and the PASER cell dictates a minimum microbunch length of about 1 μm [36,37].

Figure 5(b) presents the kinetic energy gain versus the number of microbunches. For a given amount of charge in the macrobunch and for a fixed distance between two adjacent microbunches (λ_0), the implication of changing the

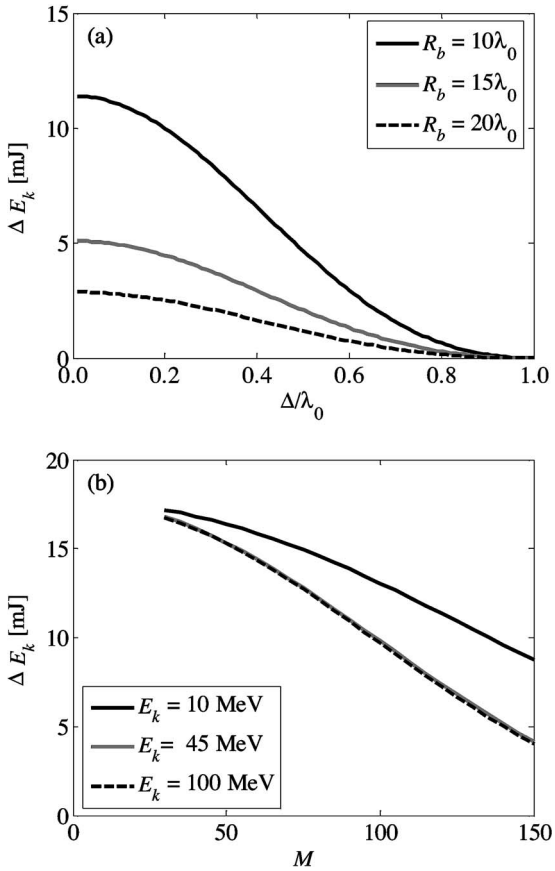

FIG. 5. (a) The macrobunch kinetic energy increase versus the length of the microbunch with R_b as a parameter, $M=90$, and $E_k=45$ MeV. (b) The macrobunch kinetic energy increase versus the number of microbunches with E_k as a parameter, $\Delta=0.1\lambda_0$, and $R_b=10\lambda_0$. In both frames, the energy density stored in the medium at the resonance frequency was set to be $w_{\mathrm{act}}=1.7$ mJ/cm^3, and the number of electrons in the macrobunch is 10^{10}.

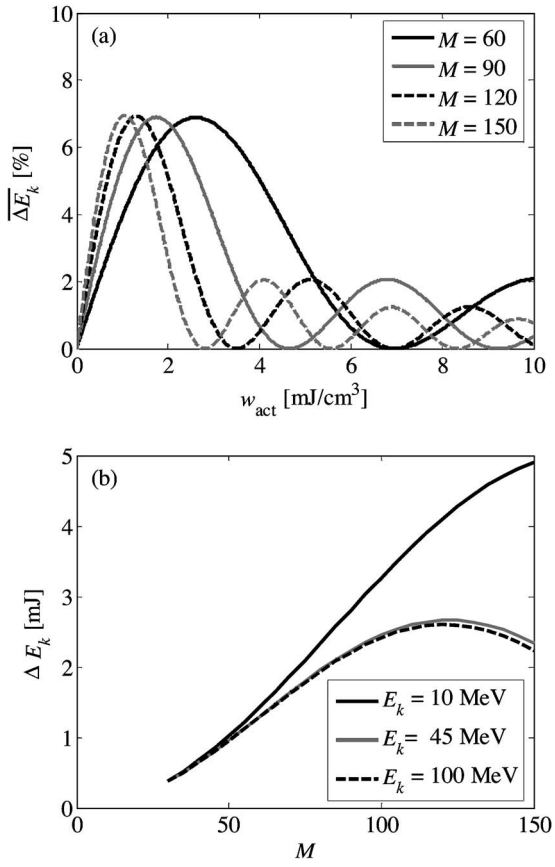

FIG. 6. (a) The relative change in the kinetic energy of the macrobunch versus the energy density stored in the medium at the resonance frequency with M as a parameter. Each single electron has a kinetic energy of 45 MeV. (b) The macrobunch kinetic energy increase versus the number of microbunches with E_k as a parameter, and $w_{\mathrm{act}}=1.7$ mJ/cm^3. In both frames, the microbunch length is $\Delta=0.1\lambda_0$, $R_b=10\lambda_0$, and the total amount of the charge in each microbunch is set to be 8 pC.

value of M is a variation in the amount of charge in each microbunch—or equivalently a change in the macrobunch's duration. Evidently, the energy gain drops as the amount of charge in each microbunch decreases. As we have already indicated, the acceleration is due to a stimulated process, and therefore, bearing in mind that the energy stored in the medium is maintained constant, the last fact is foreseen. Typically at the BNL-ATF the macrobunch may split into 80–150 microbunches.

F. Fixed charge in each microbunch

While in any practical setup the total amount of charge in the macrobunch will be readily controlled, it is instructive to examine also a regime where the amount of the charge in the microbunch is kept constant. Figure 6(a) shows the relative energy change as a function of the energy density stored in the medium at the resonance—M is a parameter. It was assumed that each microbunch consists of 5×10^7 electrons, corresponding to a charge of 8 pC, the average energy was set to be 45 MeV, the beam's radius is $10\lambda_0$, and the microbunch length was taken to be $0.1\lambda_0$. Evidently, the peak of the relative energy change is M independent, implying that for a sufficiently long train ($M\gg1$), each bunch interacts with the medium *independent* of the others.

Next, the kinetic energy gain for a given amount of charge in the microbunch versus the number of microbunches was examined, and the result is presented in Fig. 6(b) for different values of E_k. The other parameters were chosen as in Fig. 6(a) and $w_{\mathrm{act}}=1.7$ mJ/cm^3. Two facts are evident from this figure. First, for relativistic energies the energy gain is not affected by the pulse duration of the macrobunch. Second, there is an optimum pulse duration for which the increase in the kinetic energy of the macrobunch reaches its maximum. For ultrarelativistic energies this optimum ($M^{(\mathrm{opt})}$) is controlled mainly by the energy density stored in the medium. Specifically, $M^{(\mathrm{opt})}$ decreases with the increase of w_{act}.

G. Čerenkov radiation

So far, the *real* part of the dielectric coefficient at the resonance has been taken to be unity in order to emphasize the role of the active medium, ignoring in the process

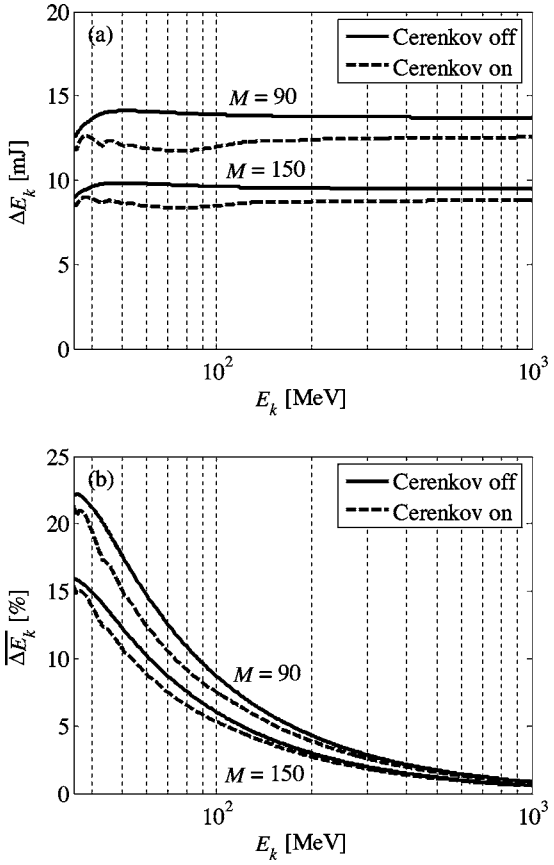

FIG. 7. (a) The macrobunch kinetic energy increase versus E_k with M as a parameter, accounting for Čerenkov radiation. (b) The relative change in the kinetic energy of the macrobunch versus E_k, accounting for Čerenkov radiation. In both cases, $R_b=10\lambda_0$, $\Delta=0.1\lambda_0$, $N_{el}=10^{10}$, and $w_{act}=1$ mJ/cm^3.

the competition from the Čerenkov radiation at high energies. Two main parameters determine the generation of this radiation: the average kinetic energy of the electrons and the gas pressure. For the given mixture and pressure, the Čerenkov radiation starts to occur for energies exceeding the 36 MeV level, since the effective refractive index is of the order of 1.0001 [38]. In Fig. 7(a) the total energy gain versus the average kinetic energy of the electrons for different M is introduced accounting for the Čerenkov radiation. These curves were calculated by numerically evaluating the integral for the energy exchange as it appears in Eq. (13). In these curves the beam radius was set to be $R_b=10\lambda_0$, $\Delta=0.1\lambda_0$, $N_{el}=10^{10}$, and $w_{act}=1$ mJ/cm^3. As revealed from this figure, it is clear that the energy gain decreases due the occurrence of the Čerenkov radiation. However, this decrease is less than 10%, in spite of the fact that the Čerenkov radiation is a broadband phenomenon. In Fig. 7(b) the relative change in the kinetic energy for the same set of parameters, as in Fig. 7(a), is introduced. Both frames indicate that for the typical parameters considered we can ignore the impact of the Čerenkov radiation.

VI. PASER EXPERIMENT

Recently, we have conducted a proof-of-principle experiment to demonstrate the PASER scheme [25]. In this section we present a detailed account of the experimental setup considerations and compare the experimental results with the theoretical predictions.

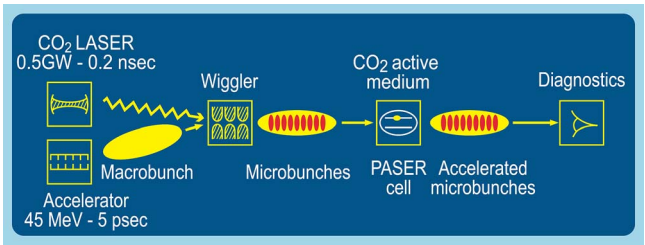

FIG. 8. (Color online) Schematic layout for the PASER experiment. The distance separating the wiggler and the PASER cell is about 2.5 m.

A. Experimental setup

The proof-of-principle experiment was carried out at the BNL-ATF, which features a photocathode-driven microwave linear accelerator and a high-peak-power CO_2 laser. A wiggler in which a laser beam interacts with a macrobunch of electrons traveling through a periodic magnet array is used to impart a sinusoidal energy modulation on the electron beam (e-beam), thereby leading to microbunching. A schematic layout of the experiment is presented in Fig. 8.

A quasimonoenergetic (45-MeV) electron macrobunch of 5 psec duration and consisting of at least 7×10^8 particles was injected into a wiggler where it was bunched into about 150 microbunches by its interaction with a high-power CO_2 laser pulse (200 psec, 0.5 GW) operating at a wavelength of 10.2 μm. A 2.5-m-long drift region separates the wiggler from the PASER cell. Along this drift region the velocity modulation emerging from the wiggler becomes a *density* modulation at the entrance to the cell. The former is controlled by the intensity of the CO_2 laser pulse, and in our particular setup a ~1.5% peak-to-peak energy modulation at the wiggler was found to generate an optimal density modulation in the PASER cell. Either stronger or weaker modulation at the wiggler leads to less than optimal modulation at the location of the interaction with the active medium and, thus, smaller acceleration. Typically, at the optimal modulation, a single macrobunch is ~1 μm long [36,37] corresponding to an ultrashort pulse of about 3 fsec. Table I lists the main parameter values of the e-beam, as well as of the laser pulse used during the experiment.

The train of microbunches enters next the PASER cell that contains a mixture of CO_2 [CO_2:N_2:He(2:2:3)], held at a pressure of 0.25 atm, activated by a discharge driven by a 130-nF low-inductance capacitor, initially charged to 30 kV. The discharge is facilitated by two 40 cm$\times$12 cm aluminum electrodes which are 2.5 cm apart. Two diamond windows, of 1 mm diameter and 2 μm thickness each, are attached to both ends of the cell in order to maintain the pressure in the cell and at the same time to allow the train to propagate through the cell—a schematic of the PASER system is illustrated in Fig. 9.

For the typical values mentioned above electrical measurements (voltage and current) of the discharge indicate that

TABLE I. PASER experimental parameters and values.

Parameter	Value
e-beam energy	44.6 MeV
e-beam intrinsic energy spread (1σ)	0.03%
e-beam charge (total pulse upstream the cell)	~0.1 nC
e-beam pulse length (macrobunch)	~5 psec
e-beam focus size, rms (upstream the cell)	200 μm
Number of microbunches in the train	~150
Laser pulse length [full width at half maximum (FWHM)]	~200 psec
Laser wavelength (CO_2 laser)	10.2 μm
Laser polarization	Linear
Laser power used for optimal modulation	~0.5 GW
Laser focal width	200 μm
Gas pressure in the PASER cell	~0.25 atm
Energy density stored at resonance (estimate)	~1 mJ/cm^3

the total energy density stored in the mixture is at the most of the order of 0.1 J/cm^3. Only a small fraction of this energy density is associated with the resonance of the CO_2 molecule at 10.2 μm. Therefore, assuming a potential efficiency (as an amplifier) of 1%, we estimate the energy density available, at 10.2 μm, to be of the order of 1 mJ/cm^3. Based on this estimate, in the volume covered by a beam of a radius of 150 μm, the available energy is of the order of 70 μJ. However, the field associated with a relativistic bunch covers an area which effectively is γ^2 larger than the geometric beam cross section. In practice, in the vertical dimension the expansion is limited by the electrode spacing, and hence, the available energy is about 200 mJ. This value should be compared to 5 mJ kinetic energy of the train.

Beyond the energy estimates, it is important to clarify also the time scales involved. As the gas mixture is excited, its population is inverted, and being in a metastable state, the population inversion decays on a time scale of milliseconds. Consequently, injecting the train of bunches with a delay of about 10 μsec from the moment the discharge was triggered ensures that, on the one hand, there is no significant change in the population inversion, whereas on the other hand, the discharge process is over since it takes an order of a microsecond. The jitter in the discharge's current is of the order of 1 μsec.

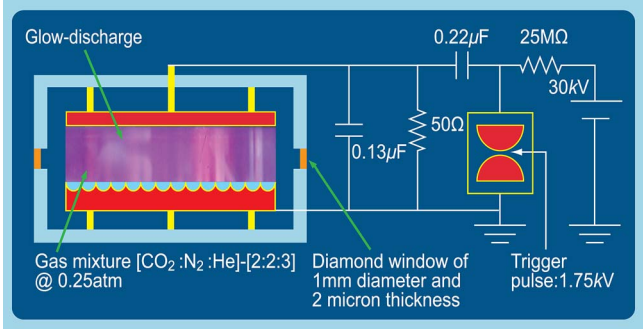

FIG. 9. (Color online) The PASER system schematic. It consists of the PASER cell and the electrical system used to excite the gas. The discharge process is triggered by a spark-gap switch ignited by a 1.75-kV pulse.

A high-resolution 8° bend magnet spectrometer, located downstream the PASER cell, was employed for detecting the resulting time-integrated energy distribution of all electrons in the e-beam. Due to various external constraints, no focusing magnetic field could be applied on the 50-cm-long PASER cell and, as a result, the internal repulsion forces, scattering in the input and output diamond windows, as well as scattering from the gas mixture, are responsible for a transmission of only 60% of the electrons; i.e., about 4×10^8 electrons were measured at the spectrometer. This is consistent with a Coulomb beam divergence of 3 mrad as evaluated theoretically.

B. Experimental results

In order to demonstrate the PASER effect, during the experiment, pairs of shots with *discharge on* and *off* were recorded for different peak-to-peak energy modulations (1%–3%). A jitter of up to 50 keV in the energy spread of the e-beam was observed at the spectrometer. As the PASER effect manifested itself as an increase of the energy spread of the macrobunch as measured at the spectrometer, in the presence of the discharge in the cell, any increase beyond the 50 keV in the energy spread is considered as an acceleration via the PASER scheme. One should keep in mind that the only other source of energy available is the laser pulse. However, we considered only pairs of shots of which the laser energy, utilized for the modulation in the wiggler, to be virtually identical, corresponding to a specific peak-to-peak energy modulation.

Figure 10 presents sample images from the spectrometer's camera; the energy dispersion is in the horizontal plane. In Fig. 10(a) the e-beam energy distribution with the discharge off is shown, while Fig. 10(b) shows the former with the discharge on. Evidently, the energy spectrum in frame (b) is broadened to the left in comparison to the spectrum in (a), corresponding to an energy increase of about 0.45%—i.e., 200 keV. Without any data processing we clearly observe the impact of the discharge on the modulated beam, and as we shall discuss subsequently, the absolute value of the energy gain is in accordance with the theoretical predictions as established based on the model described in previous sections.

The energy spectra, corresponding to the raw images of the spectrometer introduced in Fig. 10, are presented in Fig. 11. In order to facilitate a proper comparison between the two spectra, both curves were normalized to describe the density probability of finding an electron in the range $E\rightarrow E+dE$ or, in other words, the area below each one of the curves is unity. Examining the two curves we discern that the energy spectrum for discharge on is wider than that with discharge off. Moreover, the peak of higher energies in the case of discharge on is shifted towards higher energies, in comparison to the corresponding peak for discharge off. This shift is an even clearer indication for particles acceleration due to the interaction with the excited gas. Based on these curves, we evaluated the relative change in the kinetic energy

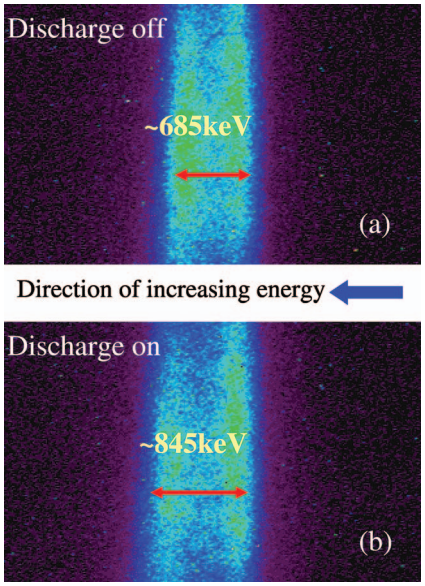

FIG. 10. (Color) Raw video images from the electron energy spectrometer. Energy dispersions is in the horizontal direction. (a) Discharge is off in the PASER cell. (b) Discharge is on in the PASER cell. In both cases, ~1.5% peak-to-peak energy modulation was imparted.

of the macrobunch (discharge on or off), estimating it to be ~0.15%, which corresponds to an increase of ~5 μJ in the kinetic energy of the macrobunch. In order to further emphasize the signature of the accelerated electrons, in Fig. 11(b) we plot the difference between the spectra presented in Fig. 11(a).

For an efficient interaction to occur it is important to have in the cell a maximum density modulation of the electrons. Altering the latter reduces significantly the acceleration process, as was illustrated in previous sections. In Fig. 12 we present the spectra of another set of shots with a peak-to-peak energy modulation of ~3% at the wiggler—which is significantly off from the value corresponding to optimal density modulation in the cell. Evidently, the energy shift (~70 keV) in this case is smaller than the one obtained for the optimal (~1.5% peak-to-peak).

C. Comparison with the 2D theory

For an adequate comparison of the experimental results with the theory developed in Secs. II–IV five parameters need to be established: (i) the effective beam radius (R_b) along the interaction length, (ii) the microbunch length, (iii) the number of electrons in each microbunch, (iv) the effective energy density stored at the resonance frequency, and finally (v) the effective interaction length (d).

We do not have *exact* values of either one of these five parameters, but we have reasonable estimates that enable us to plot the region in these parameters' space, where our system operates. The ellipse in Fig. 13 presents the range of the experimental relative change in the kinetic energy versus the estimated range of the stored energy density, the interaction length, and the beam radius. According to this estimate and

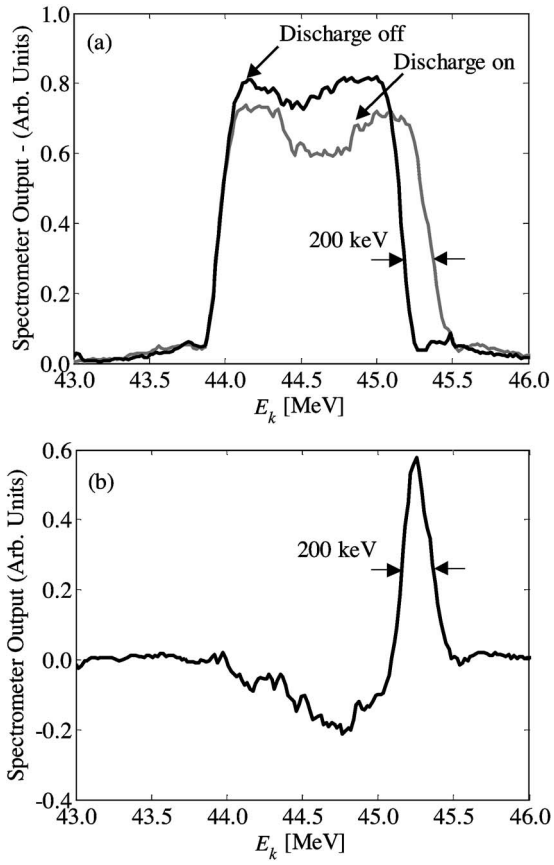

FIG. 11. The energy spectra of a single pair of shots with and without discharge and with ~1.5% peak-to-peak energy modulation. (a) Comparison of the energy spectra discharge off or on, ~200 keV energy increase is observed. (b) Energy spectra difference (discharge on minus discharge off).

relying on our model, a maximum kinetic energy gain of 0.19% is anticipated, and therefore, our experimental estimate (0.15%) is within the range predicted by the theoretical model. In what follows, we discuss the main considerations allowing us to estimate these parameters.

Macrobunch and microbunch charge. Due to partial (transverse) overlap of the e-beam with the laser pulse only about 50% of the total amount of the charge injected is actually modulated as the bunch traverses the wiggler [36,37], and therefore, at the most, 50% of the electrons collected at the spectrometer may have experienced acceleration—as our model indicates no net energy exchange is achieved in the absence of the modulation. Consequently, only about 2×10^8 of the electrons should be considered ($N_{el}=2\times10^8$). Moreover, in practice, the longitudinal distribution of the electrons within the 5-psec macrobunch is not uniform and not even Gaussian. As a matter of fact, the density at the tail (about 1 psec) is very shallow. Therefore, we considered an effective pulse duration of 4 psec, and consequently, 120 microbunches were regarded.

Microbunch length. The pulse duration of each single microbunch was determined based on coherent transition radiation (CTR) measurements conducted recently at the BNL-ATF. In these measurements, the different harmonics of the CTR were recorded. The observed CTR harmonics indicate

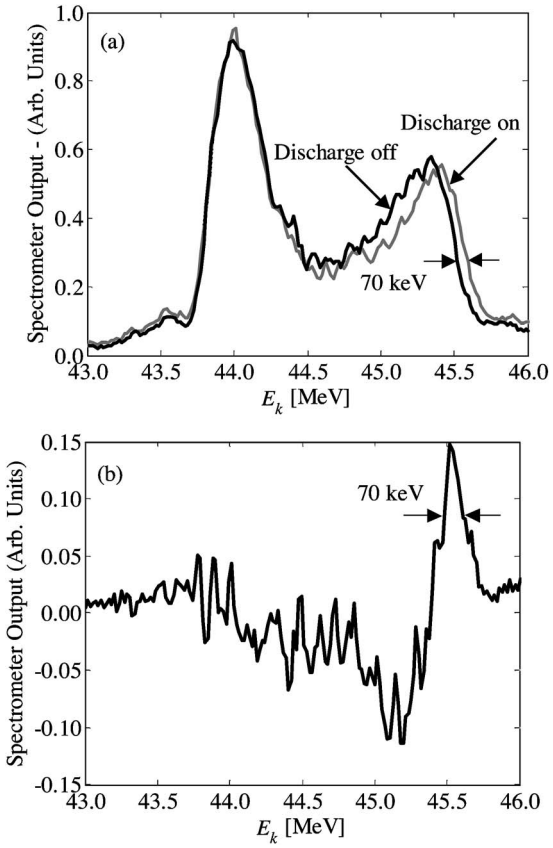

FIG. 12. The energy spectra of a single pair of shots with and without discharge, with ~3% peak-to-peak energy modulation. (a) Comparison of energy spectra discharge off or on, ~70 keV energy increase is observed. (b) Energy spectra difference (discharge on minus discharge off).

that the microbunch length may vary between 0.6 and 1.5 μm. The latter result is in good agreement with numerical simulations of the dynamics of an *e*-beam being modulated in a 45-MeV wiggler and drifts downstream the wiggler a distance of 2.5 m [36,37]. Therefore, Δ was chosen to be $0.1\lambda_0$, corresponding to ~1 μm.

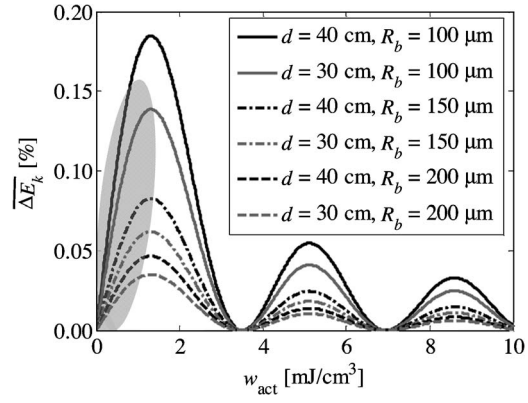

FIG. 13. The relative energy change versus the energy density stored at the resonance frequency for different radii of the macrobunch, as well as for different interaction lengths. The superimposed ellipse covers the range of the experimental results based on the estimated parameters.

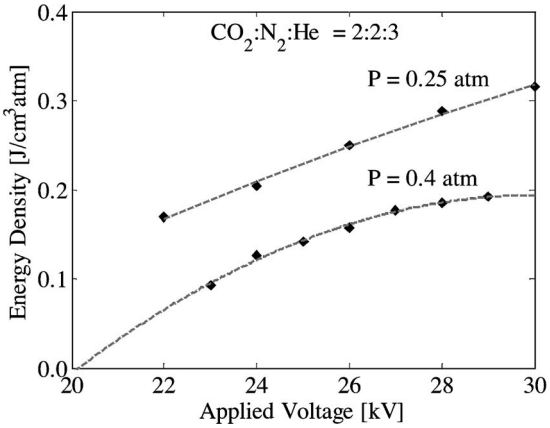

FIG. 14. The energy density stored in the excited CO_2 gas mixture versus the applied voltage used for the discharge process with the pressure, within the PASER cell, as a parameter.

Bunch radius. At the exit of the PASER cell the effective beam radius is of the order of 150–200 μm, corresponding to the *e*-beam divergence evaluated based on the multiple Coulomb scattering approximation.

Effective interaction length. The geometrical length of the electrodes that generate the discharge is 40 cm. But since the spacing is of the order of 2.5 cm, it would be reasonable to assume that edge effects may dominate the first 2.5–5.0 cm close to each one of the two ends. Consequently, an effective interaction length of 30–35 cm would be a reasonable estimate.

Stored energy density. Based on electrical measurements, the energy density stored in the excited gas within the volume of the PASER cell was estimated for different values of the applied voltage used for discharge, as well as for two distinctive gas pressures. These measurements are presented in Fig. 14. Relying on these measurements, it is obvious that for the applied voltage of 30 kV and for a pressure of 0.25 atm the total energy density stored in the gas distributed among all resonances and other scattering mechanisms is of the order of 0.1–0.2 J/cm^3. Assuming a conservative conversion efficiency of the order of 1%, if the PASER cell were to operate as a CO_2 amplifier, the energy density stored at the resonance frequency is expected to be of the order of 1–2 mJ/cm^3.

VII. SUMMARY

In the present study we have introduced a detailed account of an acceleration scheme relying on the interaction of charged particles with an active medium. The essence of this scheme is to inject into an active medium a train of microbunches being modulated at the resonance frequency of the medium. It was shown both theoretically and experimentally that energy stored in excited molecules (CO_2 gas mixture) may be transferred *directly* to a train of electron microbunches.

We developed an expression for the energy exchange, taking into account the geometry of each microbunch and describing the medium by a scalar dielectric coefficient with

TABLE II. Potential acceleration gradients for different macrobunch parameters due to its interaction with an excited CO_2 gas mixture, its main resonance being at 10.2 μm.

	$N_{el}^{(micro)}=5\times10^8$				$N_{el}^{(macro)}=5\times10^{10}$			
	$M=60$	$M=90$	$M=120$	$M=150$	$M=60$	$M=90$	$M=120$	$M=150$
Q [nC]	4.8	7.2	9.6	12	8	8	8	8
q [pC]	80	80	80	80	133	88	67	53
$w_{act}^{(opt)}$ [mJ/cm^3][a,b]	2.6	1.75	1.3	1.05	2.6	1.75	1.3	1.05
$E_{acc}^{(opt)}$ [MV/m][a,b]	62	62	62	62	103	69	52	42
$E_k^{(opt)}$[MeV][a,c]	4.1	5.1	6	6.7	4.1	5.1	6	6.7
$E_{acc}^{(opt)}(E_k^{(opt)})$ [MV/m][a,c]	100	100	100	100	165	111	82	66

[a]Values for $\Delta_0=0.1\lambda_0$.
[b]Values for $\gamma\gg1$.
[c]Values for $w_{act}^{(opt)}$.

one resonance (10.2 μm). This last assumption was demonstrated to be valid for macrobunches consisting of at least 30 microbunches. For a given resonance, we found that there is an optimal energy density for which the energy gain reaches a maximum—resulting from constructive interference of the emitted photons.

As for the impact of the macrobunch properties on the energy exchange, it was shown that the radius of the *e*-beam affects dramatically the amount of the energy gained by the train. This amount drops with the increase of the beam radius along with keeping the total charge in the macrobunch unchanged and, hence, decreasing the charge density. The energy increase is strongly dependent on the length of each microbunch—in particular, it vanishes as the length of the microbunch approaches the wavelength. Table II reveals the potential acceleration gradients corresponding to the optimal parameters as established in this study. For the CO_2 mixture it is anticipated to obtain gradients of the order of 150 MV/m. Having said that, one should bear in mind that among the challenges to be addressed in the design of future PASER experiments is the issue of gas ionization in the cell due to the high electric field generated at the beam front [40]. It is worth mentioning that in the course of our experiment no gas breakdowns were observed—this should have reflect in the current trace of the discharge. However, at higher gas pressures and higher current densities this may become a problem, although recent experiments at SLAC indicate otherwise [41].

In the second part of this study, we presented a detailed account of the PASER experiment and compared the results with the theoretical predictions. The overall gain, in the kinetic energy of a 0.1-nC 45-MeV bunch, was about 0.15%, corresponding to about 2×10^6 coherent collisions of an accelerated electron with the excited molecules of the CO_2 mixture. Furthermore, this *proof-of-principle* experiment demonstrates, for the first time, the accumulative process of coherent multiple collisions of the second kind. It also confirms that the PASER concept may be conceived as the inverse LASER effect.

ACKNOWLEDGMENTS

This study was supported by the Israel Science Foundation and the U.S. Department of Energy. The experiment was made possible by the hospitality of the Brookhaven National Laboratory and the support of the ATF peer review committee. The continuous encouragement of Ilan Ben-Zvi and the assistance and cooperation of the BNL-ATF staff directed by Vitaly Yakimenko are highly appreciated. Our discussions with Wayne D. Kimura were of great help. Our gratitude to Feng Zhou for his help during the first run of the experiment.

[1] L. Schächter, Phys. Lett. A **205**, 355 (1995).
[2] L. Schächter, Phys. Rev. E **53**, 6427 (1996).
[3] L. Schächter, Phys. Rev. E **62**, 1252 (2000).
[4] L. Schächter, E. Colby, and R. H. Siemann, Phys. Rev. Lett. **87**, 134802 (2001).
[5] L. Schächter, Phys. Lett. A **277**, 65 (2000).
[6] L. Schächter, Phys. Rev. Lett. **83**, 92 (1999).
[7] L. Schächter, in 11th Advanced Accelerator Concepts Workshop 2004, edited by V. Yakimenko, AIP Conf. Proc. No. **737** (AIP, Melville, NY, 2004), p. 715.
[8] Y. Ehrlich, C. Cohen, A. Zigler, J. Krall, P. Sprangle, and E. Esarey, Phys. Rev. Lett. **77**, 4186 (1996).
[9] A. Ting, K. Krushelnick, C. I. Moore, H. R. Burris, E. Esarey, J. Krall, and P. Sprangle, Phys. Rev. Lett. **77**, 5377 (1996).
[10] K. Krushelnick, A. Ting, C. I. Moore, H. R. Burris, E. Esarey, P. Sprangle, and M. Baine, Phys. Rev. Lett. **78**, 4047 (1997).
[11] P. Sprangle, E. Esarey, and B. Hafizi, Phys. Rev. Lett. **79**, 1046 (1997).
[12] C. I. Moore, A. Ting, K. Krushelnick, E. Esarey, R. F. Hubbard, B. Hafizi, H. R. Burris, C. Manka, and P. Sprangle, Phys. Rev. Lett. **79**, 3909 (1997).
[13] D. Gordon *et al.*, Phys. Rev. Lett. **80**, 2133 (1998).
[14] C. E. Clayton, K.-C. Tzeng, D. Gordon, P. Muggli, W. B. Mori, C. Joshi, V. Malka, Z. Najmudin, A. Modena, D. Neely, and A.

E. Dangor, Phys. Rev. Lett. **81**, 100 (1998).
[15] C. I. Moore, A. Ting, S. J. McNaught, J. Qiu, H. R. Burris, and P. Sprangle, Phys. Rev. Lett. **82**, 1688 (1999).
[16] P. Sprangle, B. Hafizi, and P. Serafim, Phys. Rev. Lett. **82**, 1173 (1999).
[17] C. E. Clayton, K. A. Marsh, A. Dyson, M. Everett, A. Lal, W. P. Leemans, R. Williams, and C. Joshi, Phys. Rev. Lett. **70**, 37 (1993).
[18] P. Chen, J. M. Dawson, R. W. Huff, and T. Katsouleas, Phys. Rev. Lett. **54**, 693 (1985).
[19] P. Chen, J. J. Su, J. M. Dawson, K. L. F. Bane, and P. B. Wilson, Phys. Rev. Lett. **56**, 1252 (1986).
[20] N. Barov, M. E. Conde, W. Gai, and J. B. Rosenzweig, Phys. Rev. Lett. **80**, 81 (1998).
[21] T. C. Chiou and T. Katsouleas, Phys. Rev. Lett. **81**, 3411 (1998).
[22] W. Gai, P. Schoessow, B. Cole, R. Konecny, J. Norem, J. Rosenzweig, and J. Simpson, Phys. Rev. Lett. **61**, 2756 (1988).
[23] J. Franck and G. Hertz, Deutsche Phys. Ges. **16**, 457 (1914).
[24] G. D. Latyscheff and A. I. Leipunsky, Z. Phys. **65**, 111 (1930).
[25] S. Banna, V. Berezovsky, and L. Schächter, Phys. Rev. Lett. **97**, 134801 (2006).
[26] R. B. Palmer, J. Appl. Phys. **43**, 3014 (1972).
[27] E. D. Courant, C. Pellegrini, and W. Zakowicz, Phys. Rev. A **32**, 2813 (1985).
[28] W. D. Kimura *et al.*, Phys. Rev. Lett. **86**, 4041 (2001).
[29] J. A. Edighoffer, W. D. Kimura, R. H. Pantell, M. A. Piestrup, and D. Y. Wang, Phys. Rev. A **23**, 1848 (1981).
[30] W. D. Kimura, G. H. Kim, R. D. Romea, L. C. Steinhauer, I. V. Pogorelsky, K. P. Kusche, R. C. Fernow, X. Wang, and Y. Liu, Phys. Rev. Lett. **74**, 546 (1995).
[31] S. J. Smith and E. M. Purcell, Phys. Rev. **92**, 1069 (1953).
[32] N. M. Kroll, in *Linear Acceleration of Particles*, edited by C. Joshi and T. Katsouleas, AIP Conf. Proc. No. **130** (AIP, New York, 1985), p. 253.
[33] *Handbook of Mathematical Functions*, edited by M. Abramowitz and I. A. Stegun (Dover Publications, New York, 1972).
[34] I. Frank and Ig. Tamm, C. R. Acad. Sci. URSS **14**, 109 (1937).
[35] A. E. Siegman, *LASERS* (University Science Books, Mill Valley, CA, 1986).
[36] W. D. Kimura *et al.*, Phys. Rev. ST Accel. Beams **4**, 101301 (2001).
[37] W. D. Kimura *et al.*, Phys. Rev. ST Accel. Beams **7**, 091301 (2004).
[38] I. S. Grigoriev and E. Z. Meylihov, *Handbook of Physical Values* (Energoatomizdat, Moscow, 1991).
[39] G. R. Lynch and O. I. Dahl, Nucl. Instrum. Methods Phys. Res. B **58**, 6 (1991).
[40] R. B. Miller, *An Introduction to the Physics of Intense Charged Particle Beams* (Plenum Press, New York, 1982).
[41] M. J. Hogan *et al.*, Phys. Rev. Lett. **95**, 054802 (2005).